Inorg. Chem. **2002**, *41*, 3091–3101

Interpretation of Indirect Nuclear Spin–Spin Coupling Tensors for Polyatomic Xenon Fluorides and Group 17 Fluorides: Results from Relativistic Density-Functional Calculations

David L. Bryce[†,‡] **and Roderick E. Wasylishen***[,†]

Departments of Chemistry, Dalhousie University, Halifax, Nova Scotia, Canada B3H 4J3, and University of Alberta, Edmonton, Alberta, Canada T6G 2G2

Received January 9, 2002

Significant improvements have been made recently in the calculation of NMR indirect nuclear spin–spin coupling tensors (**J**). In particular, the relativistic zeroth-order regular approximation density-functional theory (ZORA-DFT) approach holds great promise for the calculation of spin–spin coupling constants for a variety of chemical systems containing heavy nuclei. In the present work, the ZORA-DFT method is applied to the calculation of the complete reduced coupling tensors, **K**, for a range of chlorine-, bromine-, iodine-, and xenon-containing species: **K**(Cl,F) for ClF_2^+, ClF_3, ClF_4^+, ClF_5, ClF_6^-, and ClF_6^+; **K**(Br,F) for BrF_3, BrF_6^-, and BrF_6^+; **K**(I,F) for IF_4^+ and IF_6^+; **K**(Xe,F) for XeF^+, XeF_2, XeF_3^+, XeF_4, XeF_5^-, XeF_5^+, and XeF_7^+. These species represent a wide variety of geometrical bonding arrangements. Agreement between the calculated coupling constants and available experimental data is excellent, and the absolute sign of the coupling constants is provided. It is shown that $^1K_{iso}$ may be positive or negative even within the same molecule, e.g., $K(Cl,F)_{iso}$ may be of either sign, depending on the local environment. Periodic trends in $^1K_{iso}$ for isovalent and isostructural molecules are evident. The spin–spin coupling anisotropies, ΔK, and the orientations of the **K** tensors are also determined. The success of the calculations is a direct result of employing reliable geometries and considering both scalar and spin–orbit relativistic effects. The dependence of $K(Cl,F)_{iso}$ and $K(Xe,F)_{iso}$ on the local molecular and electronic structure is discussed in terms of the paramagnetic spin–orbit (PSO) and combined Fermi-contact spin-dipolar (FC+SD) coupling mechanisms. The PSO term depends strongly on the number of valence shell electron lone pairs on the central heavy atom, and the FC+SD contribution increases with the Cl–F or Xe–F bond length for a given series of compounds. This interpretation allows for the successful rationalization of the existing experimental data.

Introduction

Multinuclear magnetic resonance spectroscopy is of prime importance in the characterization of structure and dynamics for a wide variety of inorganic, organic, and biological species due in part to the nucleus-specific nature of this technique. NMR experiments may yield important information in the form of chemical shift (CS) tensors, indirect nuclear spin−spin coupling (**J**) tensors, and, in the case of quadrupolar nuclei ($I > 1/2$), electric field gradient (EFG) tensors.[1,2] The isotropic averages of these tensors, which are observed in solution NMR experiments, simply correspond to one-third the trace of the tensor, e.g., for the **J** tensor, J_{iso}. Solid-state NMR techniques offer the additional opportunity, under favorable circumstances, to characterize the anisotropic portion of the CS, EFG, and **J** tensors.[1,3]

From the perspective of computational chemistry, **J** tensors constitute the most challenging NMR property to calculate.[4−8]

* Author to whom correspondence should be addressed. Phone: 780-492-4336. Fax: 780-492-8231. E-mail: Roderick.Wasylishen@UAlberta.Ca.
† University of Alberta.
‡ Dalhousie University.

(1) Frydman, L. *Annu. Rev. Phys. Chem.* **2001**, *52*, 463−498.
(2) *Multinuclear NMR*; Mason, J., Ed.; Plenum Press: New York, 1987.
(3) Fyfe, C. A. *Solid State NMR for Chemists*; C.F.C. Press: Guelph, ON, 1983.
(4) Helgaker, T.; Jaszuński, M.; Ruud, K. *Chem. Rev.* **1999**, *99*, 293−352.
(5) Fukui, H. *Prog. Nucl. Magn. Reson. Spectrosc.* **1999**, *35*, 267−294.
(6) Fukui, H. In *Nuclear Magnetic Resonance: A Specialist Periodical Report*; Webb, G. A., Ed.; Royal Society of Chemistry: Cambridge, 2000; Vol. 29; Chapter 4. See also previous volumes in this series.
(7) Contreras, R. H.; Peralta, J. E.; Giribet, C. G.; Ruiz de Azúa, M. C.; Facelli, J. C. *Annu. Rep. Nucl. Magn. Reson. Spectrosc.* **2000**, *41*, 55−184.

10.1021/ic020025u CCC: $22.00
Published on Web 05/16/2002

During the past decade, however, significant theoretical advances have been made in this area.[9−19] The calculation of **J** tensors is now feasible for a variety of small systems composed of relatively light atoms using approaches based on either ab initio or density-functional theory (DFT) methods. DFT approaches to calculating NMR properties have the advantage of being able to treat relatively large systems.[20] Autschbach and Ziegler have recently implemented a zeroth-order regular approximation (ZORA) DFT method for calculating **J** tensors[21,22] which yields reliable **J** tensors for couplings involving heavy atoms such as platinum, thallium, and mercury.[23,24] Thus, the opportunity now exists for the accurate calculation and interpretation of spin−spin coupling constants involving heavy atoms.

The recent resurgence of activity and interest in noble gas chemistry[25−29] draws attention to the impact which multinuclear magnetic resonance has had on the development of this field, in particular for xenon compounds.[30] The most abundant (26.44%) NMR-active xenon nucleus, ^{129}Xe, has a nuclear spin of $^1/_2$ with a magnetic moment with magnitude slightly greater than that of ^{13}C, which has made ^{129}Xe NMR studies feasible for a wide variety of xenon compounds. Furthermore, since most xenon compounds contain fluorine (^{19}F; $I = {}^1/_2$; natural abundance = 100%), a wealth of spin−spin coupling data, $J(^{129}\mathrm{Xe},^{19}\mathrm{F})_{iso}$, exists. It has recently been demonstrated that ^{131}Xe ($I = {}^3/_2$, natural abundance = 21.1%) NMR offers the potential to obtain data which are complementary to the ^{129}Xe NMR results for xenon nuclei in high-symmetry environments, e.g., XeO_4 solutions.[29] Several empirical correlations involving $J(^{129}\mathrm{Xe},^{19}\mathrm{F})_{iso}$ have been made, e.g., with the isotropic fluorine chemical shift, or with the oxidation state of the xenon atom. Although many interpretations of $J(^{129}\mathrm{Xe},^{19}\mathrm{F})_{iso}$ have been based solely on consideration of the well-known Fermi-contact (FC) coupling mechanism, it is shown here that the spin-dipolar (SD) and paramagnetic spin−orbit (PSO) mechanisms may also play a significant, if not dominant, role.

Many polyatomic group 17 fluorides are isoelectronic or isovalent with xenon fluorides. Interest in the synthesis as well as the electronic and molecular structure of a variety of interhalogen compounds is widespread due to the large variety of molecular geometries and bonding environments which are found for these species.[31−46] Virtually every molecular geometry predicted qualitatively by the valence shell electron pair repulsion (VSEPR) theory of Gillespie[47] is represented by the halogen fluorides and the xenon fluorides.[48] A systematic investigation of the **J** tensors for the polyatomic group 17 fluorides is of interest based on the accurate ab initio and DFT results obtained for many small systems, including the diatomic group 17 fluorides.[22,49−52] For a reliable calculation of the spin−spin coupling constants involving heavy elements such as xenon, iodine, and bromine, relativistic effects must be taken into account.

In the present work, a systematic relativistic ZORA-DFT study of the complete **J** coupling tensors for a series of halogen fluorides and xenon fluorides is presented. Specifically, the chlorine−fluorine coupling tensors are calculated for ClF_2^+, ClF_3, ClF_4^+, ClF_5, ClF_6^-, and ClF_6^+, the bromine−

(8) Contreras, R. H.; Facelli, J. C. *Annu. Rep. Nucl. Magn. Reson. Spectrosc.* **1993**, *27*, 255−356.
(9) Vahtras, O.; Ågren, H.; Jørgensen, P.; Jensen, H. J. A.; Padkjær, S. B.; Helgaker, T. *J. Chem. Phys.* **1992**, *96*, 6120−6125.
(10) Nooijen, M.; Perera, S. A.; Bartlett, R. J. *Chem. Phys. Lett.* **1997**, *266*, 456−464.
(11) Enevoldsen, T.; Oddershede, J.; Sauer, S. P. A. *Theor. Chem. Acc.* **1998**, *100*, 275−284.
(12) Vaara, J.; Ruud, K.; Vahtras, O. *J. Comput. Chem.* **1999**, *20*, 1314−1327.
(13) Visscher, L.; Enevoldsen, T.; Saue, T.; Jensen, H. J. A.; Oddershede, J. *J. Comput. Chem.* **1999**, *20*, 1262−1273.
(14) (a) Malkin, V. G.; Malkina, O. L.; Salahub, D. R. *Chem. Phys. Lett.* **1994**, *221*, 91−99. (b) Malkina, O. L.; Salahub, D. R.; Malkin, V. G. *J. Chem. Phys.* **1996**, *105*, 8793−8800.
(15) Sychrovský, V.; Gräfenstein, J.; Cremer, D. *J. Chem. Phys.* **2000**, *113*, 3530−3547.
(16) Helgaker, T.; Watson, M.; Handy, N. C. *J. Chem. Phys.* **2000**, *113*, 9402−9409.
(17) Lantto, P.; Vaara, J. *J. Chem. Phys.* **2001**, *114*, 5482−5490.
(18) Auer, A. A.; Gauss, J. *J. Chem. Phys.* **2001**, *115*, 1619−1622.
(19) Enevoldsen, T.; Visscher, L.; Saue, T.; Jensen, H. J. A.; Oddershede, J. *J. Chem. Phys.* **2000**, *112*, 3493−3498.
(20) Koch, W.; Holthausen, M. C. *A Chemist's Guide to Density Functional Theory*; Wiley-VCH: Weinheim, 2000; Chapter 11.
(21) Autschbach, J.; Ziegler, T. *J. Chem. Phys.* **2000**, *113*, 936−947.
(22) Autschbach, J.; Ziegler, T. *J. Chem. Phys.* **2000**, *113*, 9410−9418.
(23) Autschbach, J.; Ziegler, T. *J. Am. Chem. Soc.* **2001**, *123*, 3341−3349.
(24) Autschbach, J.; Ziegler, T. *J. Am. Chem. Soc.* **2001**, *123*, 5320−5324.
(25) Christe, K. O. *Angew. Chem., Int. Ed.* **2001**, *40*, 1419−1421 and references therein.
(26) Seidel, S.; Seppelt, K. *Science* **2000**, *290*, 117−118.
(27) Khriachtchev, L.; Pettersson, M.; Runeberg, N.; Lundell, J.; Räsänen, M. *Nature* **2000**, *406*, 874−876.
(28) Lehmann, J. F.; Dixon, D. A.; Schrobilgen, G. J. *Inorg. Chem.* **2001**, *40*, 3002−3017.
(29) Gerken, M.; Schrobilgen, G. J. *Inorg. Chem.* **2002**, *41*, 198−204.
(30) Gerken, M.; Schrobilgen, G. J. *Coord. Chem. Rev.* **2000**, *197*, 335−395.
(31) Christe, K. O.; Zhang, X.; Sheehy, J. A.; Bau, R. *J. Am. Chem. Soc.* **2001**, *123*, 6338−6348.
(32) Schroer, T.; Christe, K. O. *Inorg. Chem.* **2001**, *40*, 2415−2419.
(33) Charkin, O. P.; Klimenko, N. M.; McKee, M. L. *Russ. J. Inorg. Chem.* **2000**, *45*, 1369−1378. Translated from *Zh. Neorg. Khim.* **2000**, *45*, 1498−1507.
(34) Pak, C.; Xie, Y.; Van Huis, T. J.; Schaefer, H. F., III. *J. Am. Chem. Soc.* **1998**, *120*, 11115−11121.
(35) Schwerdtfeger, P. *J. Phys. Chem.* **1996**, *100*, 2968−2973.
(36) Mahjoub, A. R.; Hoser, A.; Fuchs, J.; Seppelt, K. *Angew. Chem., Int. Ed. Engl.* **1989**, *28*, 1526−1527.
(37) Kaupp, M.; van Wüllen, Ch.; Franke, R.; Schmitz, F.; Kutzelnigg, W. *J. Am. Chem. Soc.* **1996**, *118*, 11939−11950.
(38) Van Huis, T. J.; Galbraith, J. M.; Schaefer, H. F., III. *Mol. Phys.* **1996**, *89*, 607−631.
(39) Buslaev, Yu. A.; Klyagina, A. P. *Coord. Chem. Rev.* **1993**, *126*, 149−175.
(40) Mahjoub, A. R.; Zhang, X.; Seppelt, K. *Chem. Eur. J.* **1995**, *1*, 261−265.
(41) Gillespie, R. J.; Schrobilgen, G. J. *Inorg. Chem.* **1974**, *13*, 1230−1235.
(42) Alexandre, M.; Rigny, P. *Can. J. Chem.* **1974**, *52*, 3676−3681.
(43) Brownstein, M.; Selig, H. *Inorg. Chem.* **1972**, *11*, 656−658.
(44) Tornieporth-Oetting, I. C.; Klapötke, T. M. *Heteroat. Chem.* **1993**, *4*, 543−552.
(45) Christe, K. O. *Inorg. Chem.* **1973**, *12*, 1580−1587.
(46) Mahjoub, A. R.; Seppelt, K. *Angew. Chem., Int. Ed. Engl.* **1991**, *30*, 323−324.
(47) Gillespie, R. J.; Hargittai, I. *The VSEPR Model of Molecular Geometry*; Allyn and Bacon: Boston, 1991.
(48) Rodger, A.; Rodger, P. M. *Molecular Geometry*; Butterworth-Heinemann: Oxford, UK, 1995; Chapter 4.
(49) Bryce, D. L.; Wasylishen, R. E. *J. Am. Chem. Soc.* **2000**, *122*, 3197−3205.
(50) Bryce, D. L.; Wasylishen, R. E.; Autschbach, J.; Ziegler, T. *J. Am. Chem. Soc.* **2002**, *124*, 4894−4900.
(51) Bryce, D. L.; Wasylishen, R. E. *J. Am. Chem. Soc.* **2000**, *122*, 11236−11237.
(52) Bryce, D. L.; Wasylishen, R. E. *J. Mol. Struct.* **2002**, *602*−*603*, 463−472.

fluorine coupling tensors are calculated for BrF_3, BrF_6^-, and BrF_6^+, the iodine−fluorine coupling tensors are calculated for IF_4^+ and IF_6^+, and the xenon−fluorine coupling tensors are calculated for XeF^+, XeF_2, XeF_3^+, XeF_4, XeF_5^-, XeF_5^+, and XeF_7^+. An analysis and interpretation of the isotropic coupling constants is founded on a comparison with available experimental data and on explicit consideration of the effects of the molecular and electronic structures on the various **J** coupling mechanisms.

Background and Theory

The indirect nuclear spin−spin coupling tensor, **J**, may be described by a 3 × 3 matrix composed of nine independent elements. The **J** interaction may be described by a Hamiltonian of the form

$$\hat{H}_J = hJ_{iso}\mathbf{I}_N\cdot\mathbf{I}_{N'} + h\mathbf{I}_N\cdot\mathbf{J}'\cdot\mathbf{I}_{N'} \quad (1)$$

where $\mathbf{I}_N$ and $\mathbf{I}_{N'}$ are the spin angular momentum vectors of the two coupled nuclei, J_{iso} is one-third the trace of the tensor, and $\mathbf{J}'$ represents the anisotropic portion of **J**.[53−56] In principle, the $\mathbf{J}'$ tensor contains a symmetric and an antisymmetric part. The antisymmetric part contains up to three independent elements, depending on the local symmetry about the coupled nuclei. The effect of the antisymmetric part of **J** has never been observed experimentally,[57] though high-level MCSCF calculations have indicated that the magnitude of its components may be comparable to the components of the symmetric portion of **J**.[51] In its principal axis system (PAS), the isotropic and symmetric parts of **J** contain a total of six independent elements which may be described alternatively by three principal components J_{ii} (ii = 11, 22, 33), such that $|J_{33} - J_{iso}| \geq |J_{11} - J_{iso}| \geq |J_{22} - J_{iso}|$, and three Euler angles which define the orientation of **J** with respect to the molecular frame of reference.[58] Use of the derived parameters ΔJ (anisotropy) and η (asymmetry) to describe the properties of **J** is also convenient:

$$\Delta J = J_{33} - (J_{11} + J_{22})/2 \quad (2)$$

$$\eta = (J_{22} - J_{11})/(J_{33} - J_{iso}) \quad (3)$$

When comparing spin pairs composed of different types of nuclei, discussion of the *reduced* coupling tensor, **K**, which is equal to $4\pi^2\mathbf{J}/\gamma_N\gamma_{N'}h$, is instructive. Here, γ_N and $\gamma_{N'}$ are the magnetogyric ratios of the coupled nuclei N and N′. The units for **K** are N A^{-2} m^{-3} or, equivalently, T^2 J^{-1}. Extensive reference will be made to values of K_{iso} and ΔK in this article.

In Ramsey's original nonrelativistic formalism describing the properties of **J** coupling, three distinct coupling mechanisms were described, all of which contribute to J_{iso}.[59,60] The first, and most widely known, is the Fermi-contact (FC) mechanism which, to a first approximation, is proportional to the product of $s_N^2(0)$ $s_{N'}^2(0)$ and the square of the *s*-bond order, $P_{s_Ns_{N'}}$, where $s(0)$ is s-electron density at nuclei N and N′, respectively. Many interpretations of spin−spin coupling constants rely on the assumption that the FC mechanism is dominant. While this is true in selected cases, e.g., most couplings involving protons, it has recently been emphasized that this is not true in general.[49−51] The second mechanism is the spin−orbital mechanism, whereby the nuclear spin angular momentum couples with the electron orbital angular momentum; this mechanism is usually further subdivided into diamagnetic (DSO) and paramagnetic (PSO) contributions. The importance of the PSO mechanism for a variety of bonding situations has been established.[49−52] Finally, there is a spin-dipolar (SD) contribution to **J** which relies on the coupling of the magnetic moments of the nuclear and electronic spins. All of these noncontact contributions depend, to a first approximation, on the expectation value of the inverse cube of the electron−nuclear distance, $\langle r^{-3}\rangle_{np}$; for group 17 and 18 nuclei the values of this parameter are particularly large.[61] The SD, DSO, and PSO mechanisms also contribute to ΔJ; however, the FC mechanism is purely isotropic. There is also a FC × SD cross term which contributes to ΔJ but not to J_{iso}.

Pyykkö developed a relativistic analogue of Ramsey's theory in 1977.[62] In this formalism, the terms in Ramsey's nonrelativistic theory are combined into a single equation, although a "contact" term may be extracted and interpreted as analogous to the FC term. The relativistic ZORA-DFT treatment used in the present work allows for a description of the coupling tensor in terms which may be considered as analogous to the original nonrelativistic terms. Additional cross terms which arise in the relativistic ZORA-DFT formalism are described in the original literature[21,22] and will be mentioned in the following section.

Computational Details

Indirect nuclear spin−spin coupling tensors were calculated using the CPL module[21,22,63,64] of the Amsterdam Density Functional program[65,66] running on an IBM RS6000 workstation or a Linux-based PC with an AMD Athlon microprocessor. The calculations are based on the relativistic ZORA-DFT implementation of Autschbach and Ziegler described in refs 21 and 22. The FC, SD, DSO, and PSO coupling mechanisms were included in the

(53) Buckingham, A. D.; Pople, J. A. *Trans. Faraday Soc.* **1963**, *59*, 2421−2430.
(54) Buckingham, A. D.; Love, I. *J. Magn. Reson.* **1970**, *2*, 338−351.
(55) Robert, J. B.; Wiesenfeld, L. *Phys. Rep.* **1982**, *86*, 363−401.
(56) Wasylishen, R. E. In *Encyclopedia of Nuclear Magnetic Resonance*; Grant, D. M., Harris, R. K., Eds.; Wiley Inc.: Chichester, U.K., 1996; pp 1685−1695.
(57) Andrew, E. R.; Farnell, L. F. *Mol. Phys.* **1968**, *15*, 157−165.
(58) Spiess, H. W. In *NMR Basic Principles and Progress*; Diehl, P., Fluck, E., Kosfeld, R., Eds.; Springer-Verlag: Berlin, 1978; Vol. 15, pp 55−214.
(59) Ramsey, N. F. *Phys. Rev.* **1953**, *91*, 303−307.
(60) Pyykkö, P. *Theor. Chem. Acc.* **2000**, *103*, 214−216.
(61) Reference 2, Chapter 3, Figure 1.
(62) Pyykkö, P. *Chem. Phys.* **1977**, *22*, 289−296.
(63) Dickson, R. M.; Ziegler, T. *J. Phys. Chem.* **1996**, *100*, 5286−5290.
(64) Khandogin, J.; Ziegler, T. *Spectrochim. Acta* **1999**, *A55*, 607−624.
(65) ADF 2000.01, Theoretical Chemistry, Vrije Universiteit, Amsterdam, http://www.scm.com.
(66) (a) Baerends, E. J.; Ellis, D. E.; Ros, P. *Chem. Phys.* **1973**, *2*, 41−51. (b) Versluis, L.; Ziegler, T. *J. Chem. Phys.* **1988**, *88*, 322−328. (c) te Velde, G.; Baerends, E. J. *J. Comput. Phys.* **1992**, *99*, 84−98. (d) Fonseca Guerra, C.; Snijders, J. G.; te Velde, G.; Baerends, E. J. *Theor. Chem. Acc.* **1998**, *99*, 391−403.

calculations. In the ZORA-DFT implementation, the FC and SD terms are not separated, and the resulting combined term is labeled "FC+SD". The FC+SD term contains a purely anisotropic FC−SD cross term, and also part of the (FC+SD)−PSO cross term. Similarly, the "PSO" term that is calculated contains the remaining part of the (FC+SD)−PSO cross term. The (FC+SD)−PSO term is exactly zero in the nonrelativistic or scalar relativistic limit where no spin−orbit coupling is present.

The DFT calculations used the VWN[67] + Becke88[68] and Perdew86[69] generalized gradient approximation (GGA) as described in ref 22. All of the calculations incorporate spin−orbit relativistic corrections in addition to scalar relativistic corrections. The triple-polarized ADF ZORA V Slater-type basis sets available within the ADF package were used. A missing 5d polarization function with exponent 1.900 was added to the iodine basis set.

For ClF_2^+, calculation of **J** tensors using the multiconfigurational self-consistent field (MCSCF) method[9] as implemented in the DALTON quantum chemistry package[70] was also feasible. A restricted active space (RAS) wave function,[71] chosen on the basis of the MP2 natural orbital occupation numbers,[72] was used: 4120 (inactive), 0000 (RAS1), 4231 (RAS2), 5342 (RAS3). Up to two electrons were allowed to be excited into RAS3, and the cc-pVQZ basis set was employed on all atoms.[73] Analogous MCSCF/RAS calculations have been reported for ClF and ClF_3.[49,51]

Most calculations are based on atomic coordinates taken from experimental geometries. For some species, especially cations and anions, several experimental geometries are sometimes available depending on a number of factors, e.g., the nature of the counterion, the temperature of diffraction data collection, and what types of corrections are made to the data. For the current work, generally a single reliable geometry has been selected for each species rather than focusing on the differences in the calculated **J** couplings obtained for slightly different structures. Furthermore, intermolecular effects on the calculated coupling tensors have not been considered; calculations have been carried out for isolated monomeric species.

The experimental geometries are from the following references: ClF_2^+ from the crystal structure for $[ClF_2]^+[RuF_6]^-$;[74] ClF_3 from ref 75; ClF_4^+ from the "predicted free" structure determined in ref 31; IF_4^+ from the X-ray crystal structure for $IF_4^+Sb_2F_{11}^-$;[76] ClF_5 as reported in ref 33; ClF_6^+, BrF_6^+, and IF_6^+ from recent X-ray diffraction data for $ClF_6^+Sb_2F_{11}^-$, $BrF_6^+Sb_2F_{11}^-$, and $IF_6^+Sb_2F_{11}^-$ by Lehmann and Schrobilgen;[77] BrF_3 from the microwave data reported in ref 78; BrF_6^- from the crystal structure for $CsBrF_6$;[36] a xenon−fluorine bond length of 1.9791 Å which was determined by rotational Raman spectroscopy was used for XeF_2;[79] XeF_3^+ from the crystal structure for $XeF_3^+SbF_6^-$;[80] a xenon−fluorine bond length of 1.94 Å was used for XeF_4;[81] XeF_5^- from the crystal structure for $N(CH_3)_4^+XeF_5^-$;[82] XeF_5^+ from the crystal structure for $[XeF_5^+]_2[PdF_6^{2-}]$.[83]

Theoretical structures were used for the following species. The bond length for XeF^+ was optimized using Gaussian 98[84] at the MP2 level with the 6-311++G** basis set on fluorine and the SDB-cc-pVQZ basis set and an effective core potential on xenon; the result is 1.8601 Å. The DHP++/BHLYP geometry for ClF_6^-, $r(Cl,F) = 1.778$ Å, of Van Huis et al. was used.[38] Finally, the DFT structure of Christe et al. for XeF_7^+ [85] was employed.

In cases where couplings to atoms which are nearly equivalent are calculated, the average values are reported. For example, in the case of ClF_6^+, the average value of $K(Cl,F)_{iso}$ is reported rather than six slightly different values.

Results and Discussion

The results of the calculations of indirect nuclear spin−spin coupling tensors for polyatomic group 17 fluorides and xenon fluorides are presented in Tables 1−3. Where possible, the calculated isotropic spin−spin coupling constants have been compared with available experimental data. There are more experimental data available for the xenon species due to the existence of the spin-$^1/_2$ ^{129}Xe isotope; there are no spin-$^1/_2$ isotopes of chlorine, bromine, and iodine. In comparing calculated and experimental coupling constants, it is important to emphasize that intermolecular effects undoubtedly influence the experimental coupling constants, since many of the NMR measurements have been carried out in solution. Solvent effects are expected to be most important when the central atom is coordinatively unsaturated. Nevertheless, a qualitative comparison of the calculated and

(67) Vosko, S. H.; Wilk, L.; Nusair, M. *Can. J. Phys.* **1980**, *58*, 1200−1211.
(68) Becke, A. D. *Phys. Rev. A* **1988**, *38*, 3098−3100.
(69) Perdew, J. P. *Phys. Rev. B* **1986**, *33*, 8822−8824; **1986**, *34*, 7406.
(70) Dalton: An electronic structure program, Release 1.0 (1997), written by T. Helgaker, H. J. Aa. Jensen, P. Jørgensen, J. Olsen, K. Ruud, H. Ågren, T. Andersen, K. L. Bak, V. Bakken, O. Christiansen, P. Dahle, E. K. Dalskov, T. Enevoldsen, B. Fernandez, H. Heiberg, H. Hettema, D. Jonsson, S. Kirpekar, R. Kobayashi, H. Koch, K. V. Mikkelsen, P. Norman, M. J. Packer, T. Saue, P. R. Taylor, and O. Vahtras.
(71) Malmqvist, P.-Å.; Rendell, A.; Roos, B. O. *J. Phys. Chem.* **1990**, *94*, 5477−5482.
(72) (a) Jensen, H. J. Aa.; Jørgensen, P.; Ågren, H.; Olsen, J. *J. Chem. Phys.* **1988**, *88*, 3834−3839. (b) Guilleme, J.; Fabián, J. S. *J. Chem. Phys.* **1998**, *109*, 8168−8181.
(73) (a) Dunning, T. H., Jr. *J. Chem. Phys.* **1989**, *90*, 1007−1023. (b) Woon, D. E.; Dunning, T. H., Jr. *J. Chem. Phys.* **1993**, *98*, 1358−1371. (c) Woon, D. E.; Dunning, T. H., Jr. *J. Chem. Phys.* **1995**, *103*, 4572−4585.
(74) Bougon, R.; Cicha, W. V.; Lance, M.; Meublat, L.; Nierlich, M.; Vigner, J. *Inorg. Chem.* **1991**, *30*, 102−109.
(75) (a) Smith, D. F. *J. Chem. Phys.* **1953**, *21*, 609−614. (b) Haubrich, S. T.; Roehrig, M. A.; Kukolich, S. G. *J. Chem. Phys.* **1990**, *93*, 121−125.
(76) Edwards, A. J.; Taylor, P. *J. Chem. Soc., Dalton Trans.* **1975**, 2174−2177.
(77) Lehmann, J. F.; Schrobilgen, G. J. Unpublished work, 2001.
(78) Magnuson, D. W. *J. Chem. Phys.* **1957**, *27*, 223−226.
(79) Brassington, N. J.; Edwards, H. G. M.; Long, D. A. *J. Chem. Soc., Faraday Trans. 2* **1978**, *74*, 1208−1213.
(80) Boldrini, P.; Gillespie, R. J.; Ireland, P. R.; Schrobilgen, G. J. *Inorg. Chem.* **1974**, *13*, 1690−1694.
(81) Ivashkevich, L. S.; Ishchenko, A. A.; Kiselev, Yu. M.; Romanov, G. V.; Sokolov, V. B.; Spiridonov, V. P. *Dokl. Phys. Chem.* **1989**, *305*, 332−335. Translated from *Dokl. Akad. Nauk SSSR* **1989**, *305*, 1396−1400.
(82) Christe, K. O.; Curtis, E. C.; Dixon, D. A.; Mercier, H. P.; Sanders, J. C. P.; Schrobilgen, G. J. *J. Am. Chem. Soc.* **1991**, *113*, 3351−3361.
(83) Leary, K.; Templeton, D. H.; Zalkin, A.; Bartlett, N. *Inorg. Chem.* **1973**, *12*, 1726−1730.
(84) Frisch, M. J.; Trucks, G. W.; Schlegel, H. B.; Scuseria, G. E.; Robb, M. A.; Cheeseman, J. R.; Zakrzewski, V. G.; Montgomery, J. A., Jr.; Stratmann, R. E.; Burant, J. C.; Dapprich, S.; Millam, J. M.; Daniels, A. D.; Kudin, K. N.; Strain, M. C.; Farkas, O.; Tomasi, J.; Barone, V.; Cossi, M.; Cammi, R.; Mennucci, B.; Pomelli, C.; Adamo, C.; Clifford, S.; Ochterski, J.; Petersson, G. A.; Ayala, P. Y.; Cui, Q.; Morokuma, K.; Malick, D. K.; Rabuck, A. D.; Raghavachari, K.; Foresman, J. B.; Cioslowski, J.; Ortiz, J. V.; Stefanov, B. B.; Liu, G.; Liashenko, A.; Piskorz, P.; Komaromi, I.; Gomperts, R.; Martin, R. L.; Fox, D. J.; Keith, T.; Al-Laham, M. A.; Peng, C. Y.; Nanayakkara, A.; Gonzalez, C.; Challacombe, M.; Gill, P. M. W.; Johnson, B. G.; Chen, W.; Wong, M. W.; Andres, J. L.; Head-Gordon, M.; Replogle, E. S.; Pople, J. A. *Gaussian 98*, revision A.7; Gaussian, Inc.: Pittsburgh, PA, 1998.
(85) Christe, K. O.; Dixon, D. A.; Sanders, J. C. P.; Schrobilgen, G. J.; Wilson, W. W. *J. Am. Chem. Soc.* **1993**, *115*, 9461−9467.

Table 1. Calculated Chlorine−Fluorine Indirect Nuclear Spin−Spin Coupling Tensors for a Series of Polyatomic Chlorine Fluorides[a,b]

molecule	J_{iso}/Hz exptl	J_{iso}/Hz calcd	ΔJ/Hz	η	$K_{iso}/10^{19}$ N A^{-2} m^{-3}	$\Delta K/10^{19}$ N A^{-2} m^{-3}	% PSO for K_{iso}	% FC + SD for K_{iso}
ClF[c]	840[d]	969	−1143	0.00	874	−1031	78	22
ClF_2^+		116	1544	0.35	104	1387	73	27
ClF_2^+ (MCSCF)		119	1066	0.16	107	956	106	−6[e]
ClF_3								
F_{eq}	(+)260[f]	216	1032	0.40	195	931	113	−13
F_{ax}	(+)260[f]	212	908	0.65	191	819	101	−1
ClF_3 (MCSCF[g])								
F_{eq}	(+)260[f]	195	769	0.19	176	693	107	−7[h]
F_{ax}	(+)260[f]	164	633	0.66	148	571	39	60[i]
ClF_4^+								
F_{ax}		−59	−362	0.12	−53	−326	193	−93
F_{eq}		−289	278	0.58	−261	251	27	73
ClF_5								
F_{ax}	(−)192[j]	−276	33	0.00	−250	30	11	89
F_{eq}	≤(+)20[j]	69	−449	0.29	63	−405	−68	168
ClF_6^-		304	72	0.00	274	65	−20	120
ClF_6^+	(−)337[k]	−344	190	0.00	−310	171	14	86

[a] For completeness, the absolute values of the ZORA-DFT antisymmetric components of **K** in the principal axis system of the symmetric part of the coupling tensor are (units 10^{19} N A^{-2} m^{-3}) 167 (ClF_2^+); 137 (F_{ax} of ClF_3); 56 (F_{ax} of ClF_4^+); 6 (F_{eq} of ClF_4^+); 0.5 (F_{eq} of ClF_5). All others are zero. [b] Experimental data are included for comparison where available. Signs given in parentheses on the experimental values are inferred from the calculated results. [c] Calculated results from ref 50. [d] Reference 102. [e] The Dalton program provides the FC and SD values independently: −111% FC and 105% SD. [f] The experimental coupling constant is a weighted average coupling to both types of fluorine in the molecule.[42] [g] MCSCF results from ref 51. [h] The Dalton program provides the FC and SD values independently: −93% FC and 86% SD. [i] The Dalton program provides the FC and SD values independently: 31% FC and 29% SD. [j] Reference 42. [k] Reference 98.

Table 2. Calculated Heavy Halogen−Fluorine Indirect Nuclear Spin−Spin Coupling Tensors for Bromine Fluoride and Iodine Fluoride Species[a,b]

molecule	J_{iso}/Hz exptl	J_{iso}/Hz calcd	ΔJ/Hz	η	$K_{iso}/10^{19}$ N A^{-2} m^{-3}	$\Delta K/10^{19}$ N A^{-2} m^{-3}	% PSO for K_{iso}	% FC + SD for K_{iso}
BrF[c]	4859[d]	5239	−5955	0.00	1844	−2096	75	25
BrF_3								
F_{eq}		1717	5668	0.36	561	1852	73	27
F_{ax}		1124	4646	0.60	367	1518	−10	110
BrF_6^+	(−)1575 to (−)1587[e]	−1398	1228	0.00	−456	401	24	76
BrF_6^-	(+)1571[f]	1663	658	0.00	543	215	−25	125
IF[c]	5730[d]	4908	−6223	0.00	2158	−2736	80	20
IF_4^+								
F_{eq}		−1572	421	0.41	−691	185	42	58
F_{ax}		−653	−1178	0.49	−287	−518	149	−49
IF_6^+		−2793	2274	0.00	−1228	1000	18	82

[a] For completeness, the absolute values of the ZORA-DFT antisymmetric components of **K** in the principal axis system of the symmetric part of the coupling tensor are (units 10^{19} N A^{-2} m^{-3}) 267 (F_{ax} of BrF_3); 127 (F_{ax} of IF_4^+); 42 (F_{eq} of IF_4^+). All others are zero. [b] Experimental data are included for comparison where available. Signs given in parentheses on the experimental values are inferred from the calculated results. [c] Calculated results are from ref 50. [d] Reference 86. [e] Reference 41. [f] Reference 40.

experimental results is possible. The calculated results are for isolated molecules, typically based on geometries obtained from solid-state crystal structures, where in some cases long-range contacts to other atoms likely differ from the structure in solution. The orientations of the calculated **K** tensors are presented in Figures 1−5.

(i) Diatomics and Triatomics. High-level MCSCF and ZORA-DFT calculations have been presented previously for ClF, BrF, and IF and shown to yield isotropic and anisotropic coupling constants which are in excellent agreement with experimental gas phase data.[22,49,50,86] Some of these results are presented in Tables 1−2 for comparison with polyatomic species. For these diatomics, the PSO term dominates the isotropic spin−spin coupling constant, at approximately 80%. As a next step, the calculated results for XeF^+, ClF_2^+, and XeF_2 are presented in Tables 1 and 3. The xenon monofluoride cation is isovalent with the diatomic interhalogens and, as such, has a **K** coupling tensor which exhibits properties similar to those found for ClF, BrF, and IF. $K(Xe,F)_{iso}$ for XeF^+ is dominated by the PSO mechanism, at 74%. Furthermore, the orientation of the coupling tensor is the same as for the interhalogens (Figure 1a,c), where the largest component of the **K** tensor does not lie along the internuclear axis, but rather perpendicular to it. The experimental values of $J(^{129}Xe,^{19}F)_{iso}$ for XeF^+ range from ±6350[87] to ±7594 Hz.[30,88,89] The calculated value, −9833 Hz, provides the sign of this coupling constant and is in reasonable agreement with the experimental values. The overestimation of J_{iso} for systems where the PSO mechanism is dominant has been established and is not unexpected in this case.[90] Finally, we note that the reduced isotropic coupling constant for XeF^+, 3127×10^{19} N A^{-2} m^{-3}, exceeds

(86) Müller, H. S. P.; Gerry, M. C. L. *J. Chem. Phys.* **1995**, *103*, 577−583.
(87) Keller, N.; Schrobilgen, G. J. *Inorg. Chem.* **1981**, *20*, 2118−2129.
(88) Holloway, J. H.; Schrobilgen, G. J.; Granger, P.; Brevard, C. *C. R. Acad. Sci. Paris, Ser. C* **1976**, *282*, 519−521.
(89) Schrobilgen, G. J.; Holloway, J. H.; Granger, P.; Brevard, C. *Inorg. Chem.* **1978**, *17*, 980−987.

Table 3. Calculated Xenon−Fluorine Indirect Nuclear Spin−Spin Coupling Tensors for a Series of Polyatomic Xenon Fluorides[a,b]

molecule	J_{iso}/Hz exptl	J_{iso}/Hz calcd	ΔJ/Hz	η	$K_{iso}/10^{19}$ N A^{-2} m^{-3}	$\Delta K/10^{19}$ N A^{-2} m^{-3}	% PSO for K_{iso}	% FC + SD for K_{iso}
XeF^+	(−)6350[c] to (−)7594[d]	−9833	10505	0.00	3127	−3341	74	26
XeF_2	(−)5579[e] to (−)5665[f]	−6038	4048	0.00	1920	−1287	48	52
XeF_3^+								
F_{eq}	(−)2384[g] to (−)2440[h]	−2386	−7604	0.26	759	2419	69	31
F_{ax}	(−)2609[g] to (−)2620[h]	−2830	−8340	0.57	900	2653	17	83
XeF_4	(−)3801[e] to (−)3913[i]	−3925	−5378	0.23	1248	1710	13	87
XeF_5^-	(−)3400[j]	−3532	−3747	0.37	1123	1191	21	79
XeF_5^+								
F_{ax}	(+)1348 to (+)1512[k]	2190	−1954	0.06	−696	621	26	74
F_{eq}	(−)143.1 to (−)193.8[k]	−398	2344	0.32	126	−742	−200	300
XeF_7^+								
F_{ax}		1432	−433	0.00	−455	138	44	56
F_{eq}		245	−939	0.52	−78	299	19	81

[a] For completeness, the absolute values of the ZORA-DFT antisymmetric components of **K** in the principal axis system of the symmetric part of the coupling tensor are (units 10^{19} N A^{-2} m^{-3}) 466 (F_{ax} of XeF_3^+); 17 (F_{eq} of XeF_3^+); 14 (F_{eq} of XeF_5^-); 24, 5, and 3 (F_{eq} of XeF_5^+). [b] Experimental data are included for comparison where available. Signs given in parentheses on the experimental values are inferred from the calculated results. [c] Reference 87 [d] Reference 88. [e] Reference 91. [f] Reference 92. [g] Reference 89. [h] Reference 96. [i] Reference 30. [j] Reference 82. [k] Reference 97.

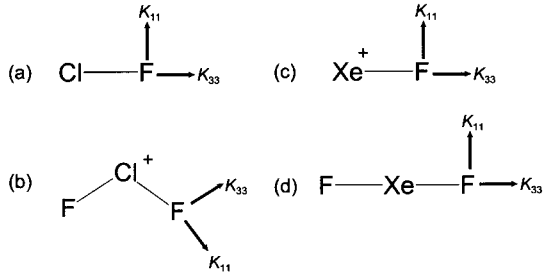

Figure 1. Calculated orientations of the chlorine−fluorine and xenon−fluorine reduced nuclear spin−spin coupling tensors for (a) ClF, (b) ClF_2^+, (c) XeF^+, and (d) XeF_2. For clarity, the coupling tensors are shown only on the fluorine nuclei. The coupling tensors for a, c, and d are axially symmetric, and so the K_{11} and K_{22} components are equivalent. For b, the K_{11} component deviates from the Cl−F bond axis by 2° and K_{22} is perpendicular to the plane of the page.

that for the isoelectronic compound IF by nearly 50%, 2158 × 10^{19} N A^{-2} m^{-3}. The same trend is evident for the reduced anisotropic coupling constant; ΔK is −3341 × 10^{19} N A^{-2} m^{-3} for XeF^+ and −2736 × 10^{19} N A^{-2} m^{-3} for IF. These increases are in accord with the periodic trends proposed for diatomic molecules in ref 49.

Results for the bent triatomic cation ClF_2^+ indicate that the PSO term is again the dominant contributor to J_{iso}. For this relatively light compound, ab initio MCSCF calculations were possible in addition to the ZORA-DFT calculations. The agreement between the two methods (Table 1) is excellent, e.g., $J(^{35}Cl,^{19}F)_{iso}$ is 135 Hz from the DFT calculation and 138 Hz from the MCSCF calculation. This agreement between two distinct computational methods lends confidence to all of the calculated spin−spin coupling tensors. Both methods indicate that the largest component of the coupling tensor in ClF_2^+ lies *along* the bond axis rather than perpendicular to it, in contrast to the result for ClF (Figure 1a,b).

For XeF_2, a linear molecule, the isotropic coupling constant is calculated to be −6038 Hz, which is in very good agreement with the experimental values which range from ±5579 Hz at 26 °C in $CFCl_3$[91] to ±5665 Hz at −68 °C in hydrogen fluoride.[30,92,93] The variation in values seems to be due primarily to solvent effects rather than temperature; Jokisaari et al. found $J_{iso}(^{129}Xe,^{19}F)$ for XeF_2 in deuterated acetonitrile to be invariant (5644.2 ± 0.6 Hz) with respect to temperature for the range 243−303 K.[94] The calculations show that J_{iso} is negative, i.e., the same sign as XeF^+. The orientation of the **K**(Xe,F) tensor is such that its largest component is perpendicular to the bond axis. It is important to note that, because of the manner in which the principal components of the **J** and **K** tensors are ordered (see Background and Theory), the label "K_{33}" simply refers to the pseudo-unique component (that which is furthest from the isotropic value) rather than to the largest component of the coupling tensor. Thus, for a linear molecule, K_{33} will always lie along the bond axis, but this does not imply that the largest component of **K** lies in this direction.

(ii) Isovalent Distorted T-Shaped Species: ClF_3, BrF_3, and XeF_3^+. The isovalent, isostructural species, ClF_3, BrF_3, and XeF_3^+, differ from the diatomics and triatomics discussed above in that there are two nonequivalent types of fluorine atoms in each structure. The ZORA-DFT data presented for chlorine trifluoride are in excellent agreement with available MCSCF data[51] and also with the experimental data.[42] It is important to note that the experimentally measured isotropic coupling, $J(^{35}Cl,^{19}F)_{iso}$ = 260 Hz, is a weighted average for the two nonequivalent fluorine sites. The ZORA-DFT calculations provide $^1J(^{35}Cl,^{19}F)_{iso}$ values of 216 and 212 Hz for the equatorial and axial fluorine atoms, respectively. Although BrF_3 is gaining recognition as a useful reagent in organic chemistry,[95] to our knowledge, no experimental data are available for comparison with the calculated coupling tensors in this compound. For XeF_3^+, the agreement with

(90) Patchkovskii, S.; Autschbach, J.; Ziegler, T. *J. Chem. Phys.* **2001**, *115*, 26−42.
(91) Birchall, T.; Myers, R. D.; de Waard, H.; Schrobilgen, G. J. *Inorg. Chem.* **1982**, *21*, 1068−1073.
(92) Gillespie, R. J.; Netzer, A.; Schrobilgen, G. J. *Inorg. Chem.* **1974**, *13*, 1455−1459.
(93) Gillespie, R. J.; Schrobilgen, G. J. *Inorg. Chem.* **1976**, *15*, 22−31.
(94) Jokisaari, J. P.; Ingman, L. P.; Schrobilgen, G. J.; Sanders, J. C. P. *Magn. Reson. Chem.* **1994**, *32*, 242−247.
(95) Rozen, S.; Ben-David, I. *J. Org. Chem.* **2001**, *66*, 496−500 and references therein.

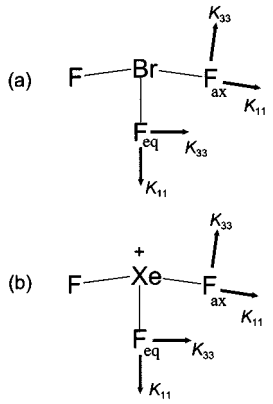

Figure 2. Calculated orientations of the bromine−fluorine and xenon−fluorine reduced nuclear spin−spin coupling tensors for the planar bent T-shaped molecules (a) BrF_3 and (b) XeF_3^+. For clarity, the coupling tensors are shown only on the fluorine nuclei. In all cases, K_{22} is perpendicular to the plane of the page. For ClF_3, identical orientations are obtained.

experiment is excellent (Table 3). The calculated isotropic coupling constant, $^1J(Xe,F_{eq})_{iso}$, for the equatorial fluorine, −2386 Hz, lies within the range determined experimentally,[30] ±2384 Hz[89] to ±2440 Hz,[96] and thus provides the sign of this coupling. The calculated value of $^1J(Xe,F_{ax})_{iso}$ for the axial fluorines, −2830 Hz, is within 10% of the experimental values, and also provides the sign of this coupling constant.

The reduced isotropic and anisotropic coupling constants for the series of distorted T-shaped molecules increase with the atomic number of the central nucleus; e.g., for the equatorial fluorine atom, $^1K_{iso}$ increases from 195×10^{19} N A^{-2} m^{-3} in ClF_3 to 561×10^{19} N A^{-2} m^{-3} in BrF_3 to 759×10^{19} N A^{-2} m^{-3} in XeF_3^+. Thus, upper and lower limits on $^1K(I,F)_{iso}$ for the equatorial fluorine atom in IF_3 may be estimated, i.e., 561×10^{19} N A^{-2} m^{-3} < $^1K(I,F_{eq})_{iso}$ < 759×10^{19} N A^{-2} m^{-3}. For all three species, the orientations of the coupling tensors are identical (Figure 2); the ZORA-DFT orientations are in agreement with the MCSCF orientation reported for ClF_3.[51] As with the linear diatomics discussed above, the largest components of the **K**(Cl,F), **K**(Br,F), and **K**(Xe,F) coupling tensors lie perpendicular to the bond axis for both fluorine sites. Finally, it is noted that, for all of the **K**(Cl,F), **K**(Br,F), and **K**(Xe,F) coupling tensors for ClF_3, BrF_3, and XeF_3^+, the anisotropy, ΔK, is consistently substantially larger than the isotropic coupling constant, K_{iso} (Tables 1−3).

(iii) Tetra-, Penta- and Heptacoordinate Species: ClF_4^+, IF_4^+, XeF_4, ClF_5, XeF_5^-, XeF_5^+, and XeF_7^+. The species discussed in this section exhibit a wide variety of geometrical arrangements and provide a rigorous test of the ability of the ZORA-DFT method to provide accurate **J** tensors for such diverse geometries. For convenience, the geometries of ClF_4^+, XeF_4, ClF_5, XeF_5^-, XeF_5^+, and XeF_7^+ are presented in Figures 3−5, along with the orientations of the calculated indirect nuclear spin−spin coupling tensors involving the central heavy atom and fluorine.

ClF_4^+ is a "seesaw" (disphenoidal) shaped cation, with two distinct types of fluorine atoms (Figure 3). The two axial

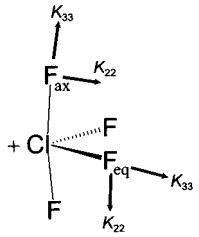

Figure 3. Calculated orientations of the chlorine−fluorine reduced nuclear spin−spin coupling tensors for the seesaw cation ClF_4^+. For clarity, the coupling tensors are shown only on the fluorine nuclei. For both types of fluorine nuclei, the K_{11} component is approximately perpendicular to the plane of the page. Analogous orientations are obtained for IF_4^+.

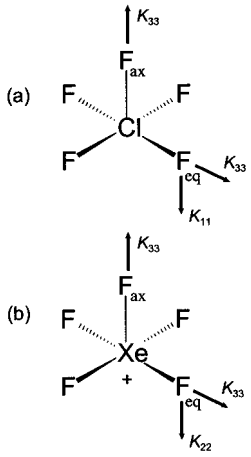

Figure 4. Calculated orientations of the chlorine−fluorine and xenon−fluorine reduced nuclear spin−spin coupling tensors for the pseudo-square pyramidal species (a) ClF_5 and (b) XeF_5^+. For clarity, the coupling tensors are shown only on the fluorine nuclei. For the unique axial fluorines, the K_{11} and K_{22} components are essentially identical. For the fluorine atoms which form a plane, note the different relative orientations of the K_{11} and K_{22} components of the Cl−F and Xe−F coupling tensors.

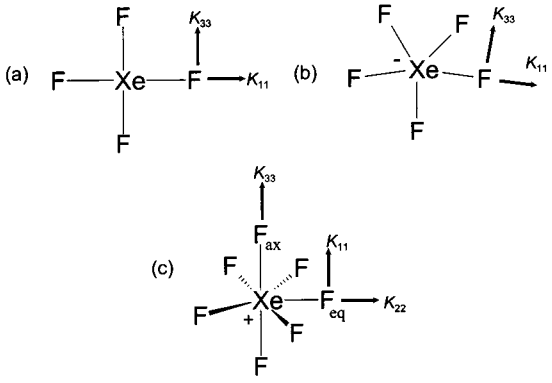

Figure 5. Calculated orientations of the xenon−fluorine reduced nuclear spin−spin coupling tensors for (a) square planar XeF_4, (b) pentagonal planar XeF_5^-, and (c) pentagonal bipyramidal XeF_7^+. For clarity, the coupling tensors are shown only on the fluorine nuclei. For both a and b, the K_{22} component of the coupling tensor lies perpendicular to the molecular plane. For the axial fluorines in c, the coupling tensor is axially symmetric. For the equatorial fluorines in c, the K_{33} component lies in the plane, and perpendicular to the Xe−F bond axis.

fluorine atoms are in a nearly linear arrangement, with an F_{ax}−Cl−F_{ax} angle of 173°.[31] Despite the similar nearly linear F_{ax}−Cl−F_{ax} arrangement found in chlorine trifluoride (175°),[75] the properties of the ^{1}**K**(Cl,F) coupling tensors in ClF_4^+ and ClF_3 are very different (Table 1). For example, $^1K(Cl,F_{ax})_{iso}$ is $+191 \times 10^{19}$ N A^{-2} m^{-3} in ClF_3 and -53×10^{19}

(96) Gillespie, R. J.; Schrobilgen, G. J. *Inorg. Chem.* **1974**, *13*, 2370−2374.

N A^{-2} m^{-3} in ClF_4^+. The reasons for such a large difference are discussed in section v, vide infra. The equatorial fluorine atoms in ClF_4^+ exhibit larger isotropic couplings, but smaller anisotropic couplings, to chlorine than do the axial fluorines. For both fluorine sites in ClF_4^+, the K_{33} component of the $^1\mathbf{K}$(Cl,F) tensor lies along the internuclear axis (Figure 3). Results analogous to those obtained for ClF_4^+ are obtained for IF_4^+ (Table 2), with an increase in the magnitude of the coupling constants. The "predicted free" seesaw structure presented by Christe et al. for ClF_4^+ is of great benefit in the present work in that the two equatorial fluorine atoms are exactly equivalent and the two axial fluorine atoms are exactly equivalent. In contrast, two sets of approximately equal coupling constants, $K(I,F_{ax})_{iso}$ and $K(I,F_{eq})_{iso}$, were obtained from calculations based on the X-ray crystal structure of $IF_4^+Sb_2F_{11}^-$;[76] the average values of these coupling constants are presented in Table 2.

In contrast to ClF_4^+, neutral xenon tetrafluoride exists in a square planar geometry (Figure 5a). There is therefore only one type of fluorine site in XeF_4 and one $^1\mathbf{K}$(Xe,F) coupling tensor. The calculated value of $^1J(^{129}Xe,^{19}F)_{iso}$, -3925 Hz, is in superb agreement with the range of experimental values, ±3801 Hz[91] to ±3913 Hz,[30] and provides the sign of the coupling constant. The PSO mechanism plays a minor role in the isotropic $^1\mathbf{K}$(Xe,F) coupling in XeF_4, representing only 13% of the total coupling. The orientation of $^1\mathbf{K}$(Xe,F) in XeF_4 is presented in Figure 5a, where the K_{22} component, which by definition is closest to K_{iso}, lies perpendicular to the molecular plane.

Chlorine pentafluoride and the xenon pentafluoride cation are isovalent and isostructural, with both compounds adopting pseudo-square pyramidal geometries (Figure 4). The reported experimental values of $^1J(^{35}Cl,^{19}F_{ax})_{iso}$ and $^1J(^{35}Cl,^{19}F_{eq})_{iso}$ for ClF_5[42] are in fair agreement with the calculated values (Table 1). As shown in Figure 4, the orientations of the chlorine−fluorine and xenon−fluorine spin−spin coupling tensors are identical. The coupling tensors involving the axial fluorines for both species are essentially axially symmetric, with the unique component lying along the internuclear axis. This is a result of the nearly perfect 4-fold symmetry about this axis. A wide variety of measurements of the two $^1J(^{129}Xe,^{19}F)_{iso}$ coupling constants in XeF_5^+ have been made.[30] For the unique axial fluorine atom in XeF_5^+, the experimental values of $^1J(^{129}Xe,^{19}F_{ax})_{iso}$ range from ±1348 to ±1512 Hz,[97] and for the equatorial fluorines, $^1J(^{129}Xe,^{19}F_{eq})_{iso}$ ranges from ±143.1 to ±193.8 Hz.[97] The calculated values of $^1J(^{129}Xe,^{19}F_{ax})_{iso}$, $+2190$ Hz, and $^1J(^{129}Xe,^{19}F_{eq})_{iso}$, -398 Hz, are in fair agreement with the experimental data, and indicate that the two coupling constants have opposing signs (Table 3). Interestingly, Gillespie and Schrobilgen have carried out double-resonance NMR experiments on XeF_5^+ which indicate that $^1J(^{129}Xe,^{19}F_{ax})_{iso}$ is of opposite sign compared to most other xenon−fluorine coupling constants.[97] The present calculations confirm this result and agree with the interpretation of Gerken and Schrobilgen,[30] i.e., most values of $^1J(^{129}Xe,^{19}F)_{iso}$ are found to be negative, while $^1J(^{129}Xe,^{19}F_{ax})_{iso}$ for XeF_5^+ is positive.

The xenon pentafluoride anion, XeF_5^-, represents the first example of a pentagonal planar species (Figure 5b). The XeF_5^- moiety exhibits D_{5h} symmetry in the crystal structure for $N(CH_3)_4^+XeF_5^-$.[82] The calculated value of $^1J(^{129}Xe,^{19}F)_{iso}$, -3532 Hz, is within 5% of the value determined for $N(CH_3)_4^+XeF_5^-$ in acetonitrile solution, ±3400 Hz.[82] Interestingly, the properties of the reduced xenon−fluorine coupling tensor in XeF_5^- are very similar to those for planar XeF_4. For example, both isotropic coupling constants are negative and of the same approximate value; the anisotropies of the coupling constants are of the same sign and order of magnitude; and the relative importance of the various coupling mechanisms is approximately constant for the two compounds, e.g., the PSO mechanism contributes 21% and 13% to the isotropic coupling constant for XeF_5^- and XeF_4, respectively (Table 3). Furthermore the orientations of $^1\mathbf{K}$(Xe,F) for both species are identical (Figure 5a,b).

The final xenon fluoride which has been studied is the hypothetical xenon heptafluoride cation. While the isoelectronic TeF_7^- species has been synthesized, the existence of XeF_7^+ has only been hypothesized.[85] To provide as complete an analysis as possible for xenon−fluorine coupling constants in a wide variety of geometrical arrangements, calculations have been carried out on XeF_7^+. This species is predicted to exist in a pentagonal bipyramidal arrangement (Figure 5c), and thus there are two distinct fluorine sites. The results of the calculations are interesting in that they predict positive values of $^1J(^{129}Xe,^{19}F)_{iso}$ for both the axial and equatorial fluorine atoms. The only other positive $^1J(^{129}Xe,^{19}F)_{iso}$ for the xenon fluorides studied herein is for the axial fluorine in XeF_5^+ (vide supra). The values for both sites in XeF_7^+, $+1432$ Hz for $^1J(^{129}Xe,^{19}F_{ax})_{iso}$ and $+245$ Hz for $^1J(^{129}Xe,^{19}F_{eq})_{iso}$, are small relative to most of the other isotropic xenon−fluorine coupling constants presented in Table 3. The anisotropies of the coupling tensors are also relatively small. The relative values of all of the reduced isotropic xenon−fluorine and chlorine−fluorine coupling constants will be discussed in more detail in section v.

(iv) Hexacoordinate Octahedral Species: ClF_6^-, ClF_6^+, BrF_6^-, BrF_6^+, and IF_6^+. For ClF_6^-, ClF_6^+, BrF_6^-, BrF_6^+, and IF_6^+, there is only one heavy-atom fluorine coupling tensor to be considered for each compound. Experimental data are present for some of these species since the central heavy halogen is in a highly symmetrical environment (very close to O_h) where the electric field gradient is approximately zero and the spin−lattice relaxation time, T_1, of the central quadrupolar nucleus is relatively long. The chlorine−fluorine, bromine−fluorine, and iodine−fluorine coupling tensors are all axially symmetric ($\eta = 0.00$) as a consequence of the high symmetry about the coupled nuclei (Tables 1 and 2). In contrast to the diatomics ClF, BrF, and IF,[22,49] the largest component of the coupling tensor for the octahedral species lies along the internuclear axis. This is due to the dominance of the PSO mechanism (~80%) for the diatomics and lack of this dominance (~20%) for the octahedral species. The isotropic and anisotropic portions of the coupling tensors are

(97) Gillespie, R. J.; Schrobilgen, G. J. *Inorg. Chem.* **1974**, *13*, 765−770.

Table 4. Selected Trends in the ZORA-DFT Isotropic Reduced Spin−Spin Coupling Constants, K_{iso}, for Isostructural Polyatomic Group 17 Fluorides and Xenon Fluorides[a]

	electron pairs[b]	coupling constant	X			
			Cl	Br	I	Xe^+
XF	4	$K(X,F)$	874	1844	2158	3127
XF_3	5	$K(X,F_{ax})$	191	367		900
		$K(X,F_{eq})$	195	561		759
XF_4^+	5	$K(X,F_{ax})$	−53		−287	*c*
		$K(X,F_{eq})$	−261		−691	
XF_5	6	$K(X,F_{ax})$	−250			−696
		$K(X,F_{eq})$	63			126
XF_6^+	6	$K(X,F)$	−310	−456	−1228	
XF_6^-	7	$K(X,F)$	274	543		

[a] All coupling constants are reported in units of 10^{19} N A^{-2} m^{-3}. All results are from spin−orbit ZORA-DFT calculations. [b] Total number of valence electron pairs around X. [c] The tetracoordinate xenon species XeF_4 is not isostructural with the group 17 fluorides XF_4^+.

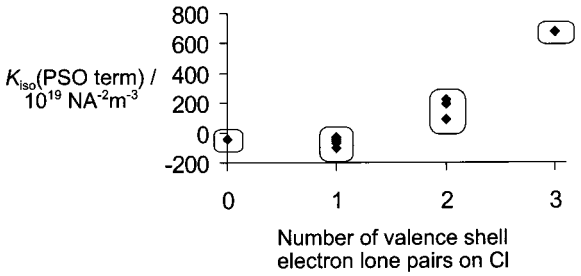

Figure 6. Plot of the calculated paramagnetic spin−orbit (PSO) contribution to the reduced chlorine−fluorine nuclear spin−spin coupling constant as a function of the number of formal valence shell electron lone pairs on the chlorine atom. Boxes are placed around the data as a guide to the approximate range covered for a particular number of lone pairs. The data are from calculations on ClF_6^+ (0 lone pair), ClF_4^+ (1 lone pair), ClF_5 (1 lone pair), ClF_6^- (1 lone pair), ClF_2^+ (2 lone pairs), ClF_3 (2 lone pairs), and ClF (3 lone pairs).

smaller for the octahedral species than for the corresponding diatomics. In general, excellent agreement is obtained between experiment and theory for the octahedral species. For example, the experimental value of $^1J(^{35}Cl,^{19}F)_{iso}$ for ClF_6^+ in hydrogen fluoride at 40 °C, ±337 Hz,[98] is overestimated by only 7 Hz.

A very interesting point is that while BrF_6^+ and BrF_6^- seem to have very similar isotropic coupling constants based on the available experimental data, $^1J(^{79}Br,^{19}F)_{iso} = \pm 1575$ Hz[41] for the cation and $^1J(^{79}Br,^{19}F)_{iso} = \pm 1571$ Hz[40] for the anion, the calculations show that in fact *these two coupling constants are of opposite sign!* The calculated values, −1398 Hz for the cation and +1663 Hz for the anion, are in very good agreement with the experimental data (Table 2). The same phenomenon is observed for ClF_6^+ and ClF_6^- (Table 1), although there are no experimental data available for the chlorine hexafluoride anion to our knowledge. The value of $^1J(^{127}I,^{19}F)_{iso}$ predicted for IF_6^+ is −2793 Hz. No evidence for J coupling in IF_6^+ was observed in the early study of $IF_6^+AsF_6^-$ of Hon and Christe,[99] perhaps due to efficient relaxation of the ^{127}I nucleus.

(v) Interpretation of the Indirect Nuclear Spin−Spin Coupling Tensors. The ZORA-DFT calculated indirect nuclear spin−spin coupling tensors discussed above are generally in very good agreement with the available experimental data. Presented in Table 4 is a summary of some of the calculated results, which serves to illustrate some of the general trends in the isotropic coupling constants involving ^{19}F coupled to a heavier halogen or to xenon. The most obvious trend is that, for a given set of isoelectronic and isostructural compounds, the value of $K(X,F)_{iso}$ (where X = Cl, Br, I, Xe) tends to increase as the atomic number of X is increased. Another important point is that $K(X,F)_{iso}$, where X is kept constant, may be either positive or negative. For example, in the case of ClF_5 and XeF_5^+, the values of $K(X,F_{eq})_{iso}$ and $K(X,F_{ax})_{iso}$ are of opposite signs for the two different types of fluorines within a single molecule.

For chlorine fluorides and xenon fluorides in particular, there exists a sufficient number of experimental isotropic coupling constants for fluorine and the heavy atom to enable an analysis of trends in these coupling constants. Furthermore, by utilizing the calculated results in combination with the experimental data, new insights into the underlying reasons behind the experimental trends may be achieved. In the present section, an interpretation of the observed trends in **K**(Cl,F) and **K**(Xe,F) coupling tensors is developed based on the combined theoretical and experimental data.

In Ramsey's original nonrelativistic formalism for the interpretation of spin−spin coupling constants,[59] the PSO mechanism accounts for the interaction of the magnetic moment of a nucleus with the magnetic field established by orbital motion of the surrounding electrons (see Background and Theory section). While empirical relationships between coupling constants and the number of lone pairs on a central atom have been discussed before,[100,101] the chlorine fluoride and xenon fluoride series discussed presently represent an excellent situation for isolating the effects of the number of valence shell electron lone pairs (in the sense of VSEPR theory[47]) on the central heavy atom. Indeed, a plot of the ZORA PSO contribution to the calculated isotropic reduced chlorine−fluorine and xenon−fluorine coupling constants versus the number of lone pairs on the central chlorine or xenon atom yields a clear-cut correlation (Figures 6 and 7). For zero or one lone pair on the central atom, the PSO contribution to $^1K_{iso}$ is roughly constant, approximately zero, and generally negative. For two lone pairs, the PSO contribution increases substantially to yield a positive contribution to $^1K(Cl,F)_{iso}$ and $^1K(Xe,F)_{iso}$. Although the number of data points is limited by the number of compounds, the PSO contribution due to two lone pairs is consistently larger than the contribution observed for zero or one lone pair. Finally, when three lone pairs reside on the central atom, the PSO contribution increases approximately 4-fold compared to the contribution from two lone pairs. A large range is observed for the xenon fluorides with three lone pairs (XeF^+ and XeF_2); nevertheless, the full range lies above the maximum PSO contribution calculated for two lone pairs (see Figure 7).

(98) Christe, K. O.; Hon, J. F.; Pilipovich, D. *Inorg. Chem.* **1973**, *12*, 84−89.
(99) Hon, J. F.; Christe, K. O. *J. Chem. Phys.* **1970**, *52*, 1960−1962.
(100) See ref 2, Chapter 4, Section 2.2.1.
(101) Gil, V. M. S.; von Philipsborn, W. *Magn. Reson. Chem.* **1989**, *27*, 409−430.
(102) Fabricant, B.; Muenter, J. S. *J. Chem. Phys.* **1977**, *66*, 5274−5277.

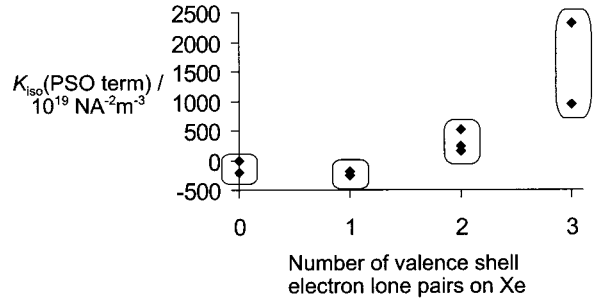

Figure 7. Plot of the calculated paramagnetic spin−orbit (PSO) contribution to the reduced xenon−fluorine nuclear spin−spin coupling constant as a function of the number of formal valence shell electron lone pairs on the xenon atom. Boxes are placed around the data as a guide to the approximate range covered for a particular number of lone pairs. The data are from calculations on XeF_7^+ (0 lone pair), XeF_5^+ (1 lone pair), XeF_5^- (2 lone pairs), XeF_4 (2 lone pairs), XeF_3^+ (2 lone pairs), XeF_2 (3 lone pairs), and XeF^+ (3 lone pairs).

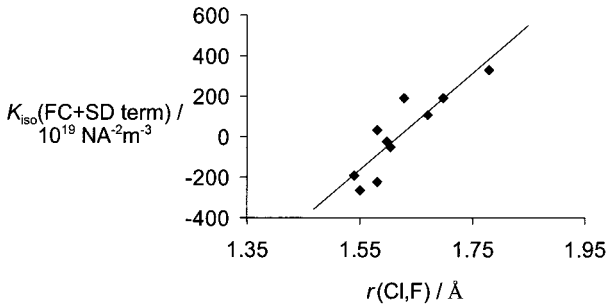

Figure 8. Plot of the calculated combined Fermi-contact + spin-dipolar (FC+SD) contribution to the reduced chlorine−fluorine nuclear spin−spin coupling constant as a function of the chlorine−fluorine bond length. See caption to Figure 6 or Table 1 for the molecules included in the plot. Linear regression provides the relationship $K(\mathrm{FC+SD})_{iso}/10^{19}$ N A^{-2} m^{-3} = 2386 (r/Å) − 3862.

The remaining contributions to the xenon−fluorine and chlorine−fluorine isotropic coupling constants arise from the Fermi-contact and spin-dipolar mechanisms. Since these two mechanisms are not separated in the ZORA-DFT formalism, the combined FC+SD term must be considered. In the nonrelativistic formalism, the FC term describes the interaction between the nuclear spin and the electron spin at the nucleus, while the SD term describes the dipolar interaction between the magnetic moment of the nucleus and the electron spin angular momentum. Whereas the PSO term depends on excited singlet state energies, the FC and SD terms both depend on excited triplet state energies, and thus there is a basis for considering the combined FC+SD term; this is done implicitly in the ZORA-DFT implementation.[21]

Shown in Figures 8 and 9 are plots of the FC+SD contribution to K_{iso} as a function of the chlorine−fluorine and xenon−fluorine internuclear distances for all of the compounds listed in Tables 1 and 3. As the plots indicate, there is a general increase in $K(\mathrm{FC+SD})_{iso}$ with the internuclear separation for a given series of compounds. Certainly the linear fits to the data are not ideal, as there is some scatter of the points about the lines of best fit. It is important to realize that this relationship with the experimental data does not imply in general that the derivative of the FC+SD term with respect to bond length is positive. Of interest is that

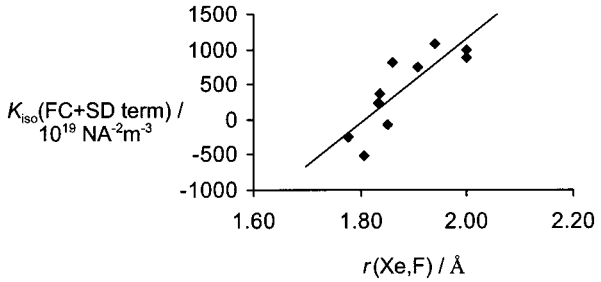

Figure 9. Plot of the calculated combined Fermi-contact + spin-dipolar (FC+SD) contribution to the reduced xenon−fluorine nuclear spin−spin coupling constant as a function of the xenon−fluorine bond length. See caption to Figure 7 or Table 3 for the molecules included in the plot. Linear regression provides the relationship $K(\mathrm{FC+SD})_{iso}/10^{19}$ N A^{-2} m^{-3} = 6021 (r/Å) − 10896.

the value of $K(\mathrm{FC+SD})_{iso}$ is negative for short bond lengths, passes through zero, and becomes positive for large bond lengths. This explains the small negative values of the total $K(\mathrm{Xe,F})_{iso}$ coupling constant for both fluorine sites in XeF_7^+, where exceptionally short Xe−F bond lengths result in a negative FC+SD contribution, and the lack of lone pairs on Xe also results in a negative PSO contribution.

From the correlations presented in Figures 6 and 7 for the PSO mechanism, and Figures 8 and 9 for the FC+SD mechanisms, all of the chlorine−fluorine and xenon−fluorine isotropic coupling constants discussed herein seem to be related to (i) the number of valence shell electron lone pairs on the central atom and (ii) the chlorine−fluorine or xenon−fluorine bond length. For the diatomics ClF and XeF^+, for example, bond lengths of intermediate value result in an intermediate contribution from the FC+SD mechanism; however, since Cl and Xe possess three lone pairs, the isotropic coupling constants for these diatomics are larger than for any of the polyatomic species. It should be noted that molecular charge has no *direct* effect on any of the coupling constants discussed herein. For example, the difference in the sign of the isotropic chlorine−fluorine coupling constants for ClF_6^+ and ClF_6^- arises primarily due to the relatively vast difference in the Cl−F bond lengths in these compounds: an average of 1.55 Å for the cation, and 1.778 Å for the anion. The value of K_{iso} for both of these species is dominated by the FC+SD contribution, which is negative at 1.55 Å and positive at 1.778 Å (Figure 8). The relationships presented in Figures 6−9 should apply equally well to the analogous series of bromine fluorides and iodine fluorides.

Conclusions

The present work has extended the application of the ZORA-DFT computational method for the calculation of **J** coupling tensors to include a variety of polyatomic species of diverse geometries. The chlorine−fluorine, bromine−fluorine, iodine−fluorine, and xenon−fluorine indirect nuclear spin−spin coupling constants have been calculated and interpreted for a large number of chemical species. Overall, the agreement between the calculated and experimental isotropic spin−spin coupling constants is excellent. The importance of employing accurate geometries for these calculations cannot be overemphasized. Recent calculations

have demonstrated the large dependence of K_{iso} and ΔK on internuclear separation for interhalogen diatomics.[50]

The incorporation of solvent effects into the calculations may provide even better agreement with experiment.

Several trends in the isotropic coupling constants have been elucidated. Investigation of the complete calculated coupling tensors for a series of seven chlorine fluorides and seven xenon fluorides has allowed for the interpretation of the heavy atom−fluorine isotropic coupling constants for these species in terms of the ZORA paramagnetic spin−orbit and combined ZORA Fermi-contact + spin-dipolar mechanisms. In particular, it has been demonstrated that a correlation exists between the number of lone electron pairs on the central heavy atom and the value of the PSO contribution to the reduced isotropic coupling constant, K_{iso}. Similarly, the value of the FC+SD term seems to increase approximately linearly with the separation between the central heavy nucleus and the fluorine nucleus for a given series of compounds. By considering both of these contributions to the total value of $K(Xe,F)_{iso}$ and $K(Cl,F)_{iso}$, the experimental data have been rationalized. The absolute sign of the coupling constants has been assigned. The analysis holds the potential to be extended to a variety of bromofluorides and iodofluorides.

The experimentalist should be aware that J_{iso} values may have opposite signs for compounds which may seem to be closely related; this may lead to an incorrect interpretation of trends in the coupling constants. For example, $K(Cl,F)_{iso}$ may be of either sign even within the same molecule (e.g., $K(Cl,F_{ax})_{iso}$ and $K(Cl,F_{eq})_{iso}$ in ClF_5 are of opposite sign) and in closely related molecules (e.g., $K(Cl,F_{ax})_{iso}$ in ClF_5 and ClF_6^- are of opposite sign). In general, it must be emphasized that reduced coupling constants for halogen−halogen or halogen−noble gas spin pairs may be either positive or negative, and may be relatively small or large in magnitude.

In many cases, indirect nuclear spin−spin coupling tensors involving fluorine are highly anisotropic. For the series ClF_3, BrF_3, XeF_3^+, the ratio $\Delta K/K_{iso}$ may be as large as 4.8; the relatively large values of ΔK for these species arise due to large anisotropic PSO contributions. In general, this ratio is much closer to unity for the other group 17 fluorides and xenon fluorides.

In conclusion, it is apparent that the ZORA-DFT method is well-suited for the prediction and interpretation of NMR spin−spin coupling constants for moderately sized polyatomic systems containing relatively heavy atoms. In particular, xenon is a heavy fifth-row atom for which relativistic effects must be considered. The agreement between experiment and theory reported in this work is partly a consequence of considering both scalar and spin−orbit relativistic corrections to the computed coupling tensors. This work also reinforces the need to calculate all contributions to the coupling tensors.

Acknowledgment. The authors thank the solid-state NMR group at the University of Alberta for many helpful comments. We are grateful to Dr. Jochen Autschbach and Professor Tom Ziegler for invaluable assistance with the CPL module for ZORA-DFT calculations. John F. Lehmann and Professor Gary Schrobilgen are thanked for providing the X-ray structures of $ClF_6^+Sb_2F_{11}^-$, $BrF_6^+Sb_2F_{11}^-$, and $IF_6^+Sb_2F_{11}^-$ in advance of publication. We thank the Natural Sciences and Engineering Research Council (NSERC) of Canada for research grants. R.E.W. is a Canada Research Chair in Physical Chemistry at the University of Alberta and thanks the University of Alberta for support. D.L.B. thanks NSERC, Dalhousie University, the Izaak Walton Killam Trust, and the Walter C. Sumner Foundation for postgraduate scholarships.

IC020025U